Chinese Chemical Letters 34 (2023) 107903

Contents lists available at ScienceDirect

Chinese Chemical Letters

journal homepage: www.elsevier.com/locate/cclet

Covalent coupling promoting charge transport of CdSeTe/UiO-66 for boosting photocatalytic CO_2 reduction

Lisha Chen[a], Qianqian Tang[b], Shihao Wu[b], Longshuai Zhang[b,*], Lifang Feng[b], Yuan Wang[c], Yiling Xie[c], Yan Li[c], Jian-Ping Zou[a,b,*], Sheng-Lian Luo[a,b]

[a] Key Laboratory of Poyang Lake Environment and Resource Utilization of Ministry of Education, School of Resources & Environment, Nanchang University, Nanchang 330031, China
[b] Key Laboratory of Jiangxi Province for Persistent Pollutants Control and Resources Recycle, Nanchang Hangkong University, Nanchang 330063, China
[c] School of Chemistry & Molecular Engineering, East China University of Science and Technology, Shanghai 200237, China

ARTICLE INFO

Article history:
Received 20 July 2022
Revised 21 September 2022
Accepted 10 October 2022
Available online 14 October 2022

Keywords:
Covalent coupling
CO_2 reduction
MOFs
Quantum dots
Photocatalytic

ABSTRACT

Quantum dots (QDs) based heterojunction is a candidate for the photocatalytic CO_2 reduction, owing to the large extinction coefficient and easy modification of band structures. However, the van der Waals interaction causes the large charge resistance and strong recombination centers between QDs and host materials, which makes the poor photocatalytic performance. Herein, a covalent bonded CdSeTe QDs and NH_2-UiO-66 heterojunction (NUC-x) is constructed through an acylamino (-CONH-). The results indicate that the acylamino between NH_2-UiO-66 and CdSeTe QDs can serve as the transfer channels for the photogenerated charges and stabilize the QDs. The optimized NUC-1200 achieved a CO generation rate of 228.68 μmol/g, which is 13 and 4 times higher than that of NH_2-UiO-66 and CdSeTe QDs, respectively. This work provides a new avenue for efficient and stable photocatalysis of QDs.

Photocatalytic CO_2 reduction to fuels is an ideal way to solve the energy crisis and greenhouse effect [1,2]. Many semiconductor photocatalysts had been developed for CO_2 reduction [3,4]. Quantum dots (QDs) are excellent candidates for photocatalytic CO_2 reduction due to their quantum confinement effect [5,6], large extinction coefficient [7,8], and easy modification of band structure [9]. And a lot of QDs photocatalysts had been developed, such as CdSe [10,11], $CsPbBr_{1.5}Cl_{1.5}$ [12], and Bi_2WO_6 [13–15]. However, the high surface energy and stabilizer of QDs cause poor stability and charge transfer [16,17]. Hence, the QDs photocatalysts need to be dispersed and stabilized.

The QDs-based heterojunction is an effective approach, which could disperse and stabilize QDs by the interaction between QDs and the support [18,19]. The CdSe QDs/g-C_3N_4 heterojunction showed improved photocatalytic stability [20,21]. And the good dispersion of CdSe QDs increased the photocatalytic activity [22,23]. However, most of the QDs-based heterojunction were linked by weak electrostatic interactions or/and van der Waals forces [24], which were not strong enough during the complex photocatalytic reactions [25]. In addition, the weak interactions between QDs and the support cause the high charge transfer barriers and easy recombination of photogenerated charges. Researchers have found that the chemical bonds linked heterojunction have better photocatalytic stability and activity. For example, the covalent-bond linked MOF/COF composites showed improved photogenerated charges transfer/migration and photocatalytic durability [26–29]. The semi-chemical interaction of Pt and g-C_3N_4 can improve the photocatalytic H_2 evolution obviously, due to the fast charge transfer channels from the strong chemical bond [30]. Therefore, it is urgent to establish strong interactions between QDs and support for fast and efficient transfer of photogenerated charges.

Metal-organic frameworks (MOFs) are ideal supports for stabilizing QDs, own to the abundant functional groups and large surface area [31]. UiO-66(Zr) is a semiconductor [32–35], which can modified by organic ligands to increase the adsorption capacity of UiO-66 for CO_2 and broaden the spectral adsorption range [31,36]. Herein, a new covalent-bonded QDs/MOFs heterojunction was successfully prepared by acylamino crosslinking. The CdSeTe QDs and NH_2-UiO-66 were crossed by the acylamino (-CONH-), which was formed through amide condensation of –COOH of CdSeTe QDs and $–NH_2$ of NH_2-UiO-66, to form CdSeTe QDs/NH_2-UiO-66 composites (NUC-X, X: the additive amount of CdSeTe QDs). The experimental results illustrated that the acylamino can act as a bridge for electron transmission and the NH_2-UiO-66 can act as electron

* Corresponding authors.
E-mail addresses: Zhang1990@163.com (L. Zhang), zjp_112@126.com (J.-P. Zou).

https://doi.org/10.1016/j.cclet.2022.107903
1001-8417/

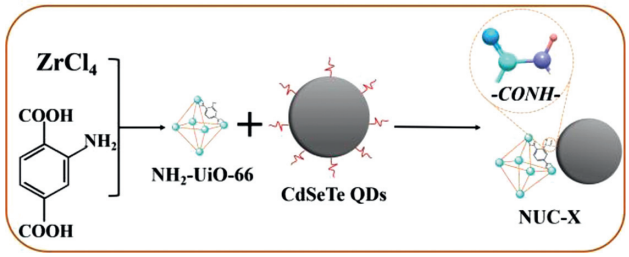

Scheme 1. Schematic illustration of the preparation of NUC-X.

traps, which can effectively promote migration and suppress recombination of photogenerated electron-hole pairs. Compared with NH_2-UiO-66, CdSeTe QDs, and the van der Waals heterostructure of NH_2-UiO-66 and CdSeTe QDs, the obtained NUC-Xs had better photocatalytic activity and stability for photocatalytic CO_2 reduction.

The NUC-X was prepared by a simple acid-assisted amide condensation reaction (Scheme 1). As shown in Fig. 1a, NUC-1200 exhibited similar diffraction peaks compared to NH_2-UiO-66, suggesting that the structure of NH_2-UiO-66 remained after the amide condensation with CdSeTe QDs. The FTIR spectra of the NUC-1200 and NH_2-UiO-66 showed similar peaks in the region of 3342–3500 cm^{-1} (Fig. S1 in Supporting information), which can be attributed to the $-NH_x$ fraction [37]. And the weaker $-NH_x$ intensity of NUC-1200 than NH_2-UiO-66 proved the reduction of $-NH_2$, which was consumed by the amide condensation. As shown in Fig. 1b, the FTIR spectra of the obtained CdSeTe QDs showed a peak centered at 1582 cm^{-1} which is consistent with –COOH from the terminal of mercaptopropionic acid [38]. And NUC-1200 showed a distinct peak at 1685 cm^{-1}, which can be assigned to the stretching band of acylamino [39]. These results indicated that the $-NH_2$ of NH_2-UiO-66 and the –COOH of CdSeTe QDs successfully formed the acylamino to obtain NUC-1200. In addition, the NUC-1200 showed similar FT-IR peaks as NH_2-UiO-66, suggesting that the condensation had not changed the structure of NH_2-UiO-66, which is consistent with the XRD results.

The surface chemical composition and electronic states of NH_2-UiO-66 and NUC-1200 were studied by XPS. Both NH_2-UiO-66 and NUC-1200 have the characteristic peaks corresponding to C, N, O,

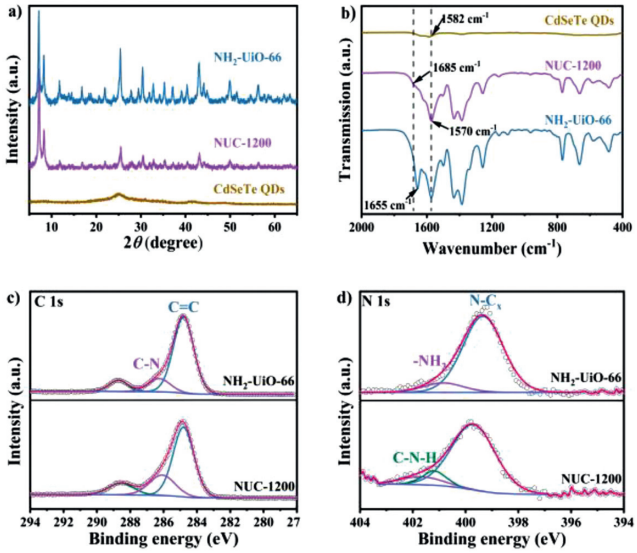

Fig. 1. (a) XRD spectra for NH_2-UiO-66, CdSeTe QDs and NUC-1200. (b) FTIR spectra for NH_2-UiO-66, CdSeTe QDs and NUC-1200. XPS spectra of (c) C 1s in NH_2-UiO-66 and NUC-1200. (d) N 1s in NH_2-UiO-66 and NUC-1200.

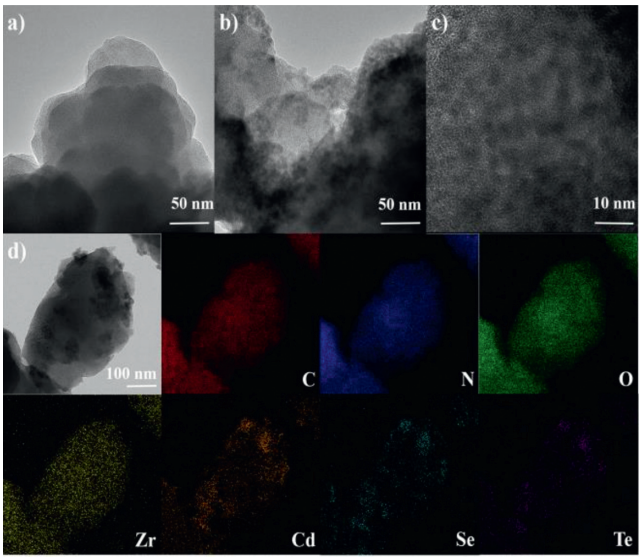

Fig. 2. TEM image of the (a) NH_2-UiO-66, (b, c) NUC-1200, the black dots are CdSeTe QDs; and (d) TEM with elemental mapping images of NUC-1200.

and Zr elements, while the presence of three other elements of Cd, Se, and Te in the obtained NUC-1200 (Fig. S2 in Supporting information). This also indicated that CdSeTe QDs and NH_2-UiO-66 were successfully combined. The high-resolution C 1s spectrum of NH_2-UiO-66 has three main peaks located at 284.8, 286.3, and 288.7 eV (Fig. 1c), corresponding to C=C, C–N (C–NH_2), and C=O, respectively [40]. Compared with NH_2-UiO-66, the C–N (286.1 eV) in NUC-1200 had a stronger intensity and smaller bonding energy, indicating the formation of acylamino. The N 1s spectrum of NH_2-UiO-66 can be deconvolved into two peaks located at 399.2 and 400.5 eV (Fig. 1d), which correspond to the tertiary nitrogen (N–C_x) and $-NH_2$ groups, respectively [41]. For the NUC-1200, a new peak centered at 401.1 eV is attributed to the C–N from covalent amide linkage and the bonding energies of N 1s were bigger than that of NH_2-UiO-66, which can be assigned to the decrease of electron density around N atoms due to the successful formation of the acylamino [42]. These results proved the strong interaction between NH_2-UiO-66 and CdSeTe QDs and the successful construction of acylamino crosslinking. The increased intensity of the –OH peak in the O 1s spectrum of NUC-1200 indicated the successful introduction of CdSeTe QDs (Fig. S3 in Supporting information). The Zr 3d spectra of NH_2-UiO-66 and NUC-1200 both have two peaks at 185.2 and 182.8 eV, which can be attributed to Zr $3d_{5/2}$ and Zr $3d_{3/2}$ (Fig. S4 in Supporting information), respectively [43].

The morphology of the as-prepared samples was investigated by transmission electron microscopy (TEM). As shown in Fig. S5 (Supporting information), the synthesized CdSeTe QDs were uniform particles with a size of 5.2 nm. For NH_2-UiO-66, a typical crystal stacking structure with a smooth surface was observed (Fig. 2a). The TEM images of NUC-1200 indicate that CdSeTe QDs were uniformly distributed on the surface of NH_2-UiO-66 (Figs. 2b and c). Although the NH_2-UiO-66 in NUC-1200 was almost indistinguishable, the particle morphology of CdSeTe QDs changed slightly after binding with NH_2-UiO-66, suggesting that NH_2-UiO-66 combined with a certain amount of CdSeTe QDs through covalent bonding. The spatial distribution of different elements in NUC-1200 was investigated by elemental mapping analysis [44]. These results indicated that the CdSeTe QDs were uniformly distributed on the surface of NH_2-UiO-66 (Figs. 2b and d).

The photo-electrochemical properties of the prepared samples were also investigated. As shown in Fig. 3a, the NUC-1200 had a lower PL intensity than that of NH_2-UiO-66 indicating that the acy-

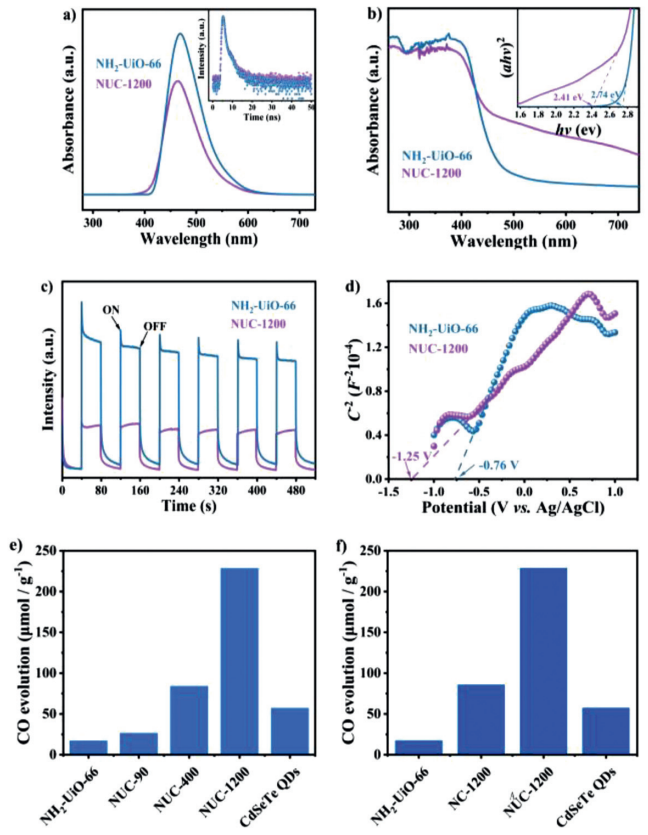

Fig. 3. (a) Steady-state photoluminescence spectra and time-resolved photoluminescence decays spectra of NH_2-UiO-66 and NUC-1200. (b) UV–vis diffuse reflectance spectra of NH_2-UiO-66 and NUC-1200. (c) Transient photocurrent responses spectra of NH_2-UiO-66 and NUC-1200. (d) Mott-Schottky spectra of NH_2-UiO-66 and NUC-1200. Photocatalytic performance (e) comparison of NH_2-UiO-66, CdSeTe QDs and NUC-X composites, (f) comparison of NH_2-UiO-66, CdSeTe QDs, NC-1200 and NUC-1200 composites.

lamino in NUC-1200 can transfer the photogenerated charges fast and inhibit recombination [45,46]. As can be seen in Fig. 3b, the NUC-1200 had a stronger UV–vis adsorption intensity than NH_2-UiO-66 in the region of 450–750 nm, indicating the enhanced light absorption capacity. Furthermore, the smaller band gap of NUC-1200 (2.41 eV) than that of NH_2-UiO-66 (2.74 eV) making it an extended light absorption range (inset in Fig. 3b). As shown in Fig. 3c, the transient photocurrent intensity of NUC-1200 was much higher than NH_2-UiO-66, which can be assigned to the faster transfer and separation of photogenerated carriers between NH_2-UiO-66 and CdSeTe QDs [47]. The flat band potential energy of NH_2-UiO-66 and NUC-1200 were −0.76 and −1.26 V *vs.* Ag/AgCl respectively (Fig. 3d). Since the flat band potential of n-type semiconductors is equal to the Fermi level [48], the Fermi levels of NH_2-UiO-66 and NUC-1200 were −0.15 and −0.65 V *vs.* RHE, respectively. Based on this, the CB of NH_2-UiO-66 and NUC-1200 can be calculated to be −0.35 and −0.85 V, respectively [37]. The matched band potential between NH_2-UiO-66 and CdSeTe QDs allows photogenerated carriers to be effectively separated.

The photocatalytic CO_2 reduction measurements of the as-prepared catalysts had been performed. The catalysts were dispersed in acetonitrile aqueous solution (acetonitrile:water = 4:1), while triethanolamine (TEOA) was the electron donor and tris(2,2′-bipyridine)ruthenium(II) chloride hexahydrate ($C_{30}H_{24}Cl_2N_6Ru$-$6H_2O$) as the photosensitizer. In Fig. 3e, the NH_2-UiO-66 exhibited the poorest photocatalytic CO evolution rate, while the NUC-Xs showed a better CO evolution rate, indicating that CdSeTe QDs

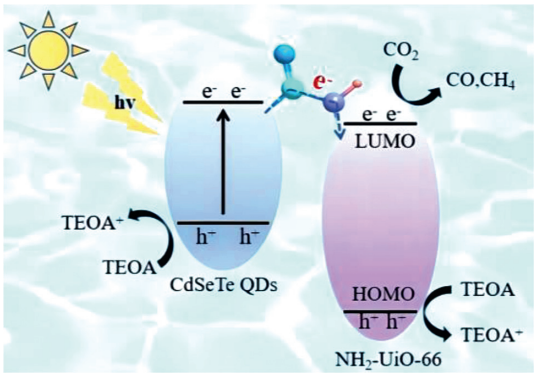

Scheme 2. Photocatalytic mechanism of the charge transfer for CO_2RR over the NUC-1200 under light irradiation.

played an important role. Among NUC-Xs, the optimized NUC-1200 achieved a CO evolution rate of 228.68 μmol/g, which was 13 and 4 times higher than NH_2-UiO-66 and CdSeTe QDs, respectively. The comparison of the photocatalytic performances were also made between this work and some related works (Table S1 in Supporting information), which proved the superior performance of NUC-1200. To further explore the effect of acylamino on photocatalytic activities, NC-1200 was constructed by van der Waals interaction between NH_2-UiO-66 and CdSeTe QDs. As shown in Fig. 3f, NC-1200 had a much lower CO evolution rate (85.7 μmol/g) compared with NUC-1200 (228.68 μmol/g). Therefore, this enhanced photocatalytic performance of NUC-1200 can mainly be attributed to the formation of acylamino. In addition, NUC-1200 showed good stability after 7 cycles owing to the strong interaction (Fig. S6 in Supporting information).

Based on the above results, the photocatalytic enhanced mechanism of NUC-1200 was proposed (Scheme 2). Firstly, NH_2-UiO-66 was linked with CdSeTe QDs by covalent bonding, thus allowing the rapid electron transfer between MOFs and QDs *via* acylamino. Then, the matched band structure between NH_2-UiO-66 and CdSeTe QDs facilitated the transfer of photogenerated electrons from the CdSeTe QDs to the CB of NH_2-UiO-66 *via* amide-bonded bridges. Finally, the covalent bonding can significantly improve the stability of heterojunction photocatalysts.

In conclusion, we had developed a novel covalent bonding heterojunction photocatalysts by a simple amide condensation. The characterization results confirmed the presence of acylamino in the synthesized NUC-Xs. Experimental results showed that the photogenerated electrons generated on CdSeTe QDs can be transferred to NH_2-UiO-66 and used for photocatalytic CO_2RR. At the same time, the acylamino served as an electron transfer bridge between NH_2-UiO-66 and CdSeTe QDs for the transfer and separation of photogenerated carriers. As a result, the obtained NUC-1200 had a better photocatalytic CO_2RR performance. This work provides a new perspective for the design and development of novel heterojunction photocatalysts.

Declaration of competing interest

The authors declare that they have no known competing fi-financial interests or personal relationships that could have appeared to inflfluence the work reported in this paper.

Acknowledgments

We gratefully acknowledge the financial support of the National Natural Science Foundation of China (Nos. 52100186 and 52170082), the Natural Science Foundation of Jiangxi Province (No. 20212ACB203008).

References

[1] X.B. Li, C.H. Tung, L.Z. Wu, Angew. Chem. Int. Ed. 58 (2019) 10804–10811.
[2] S.Q. Gong, X. Teng, Y.L. Niu, et al., Appl. Catal. B: Environ. 298 (2021) 120521.
[3] X.D. Li, Y.F. Sun, J.Q. Xu, et al., Nat. Energy 4 (2019) 690–699.
[4] J.L. White, M.F. Baruch, J.E. Pander III, et al., Chem. Rev. 115 (2015) 12888–12935.
[5] Y.E. Panfil, M. Oded, U. Banin, Angew. Chem. Int. Ed. 57 (2018) 4274–4295.
[6] L. Shi, X.H. Ren, Z.X. Zhang, et al., J. Catal. 401 (2021) 271–278.
[7] D.Y. Wang, Y.Y. Yin, C.W. Feng, et al., Catalysts 11 (2021) 275.
[8] S.C. Zhu, S. Li, B. Tang, et al., J. Catal. 404 (2021) 56–66.
[9] J.D. Wang, H.R. Ning, J. Wang, et al., ACS Appl. Nano Mater. 5 (2022) 5617–5624.
[10] H.J. Peng, P.Q. Zheng, H.Y. Chao, RSC Adv. 10 (2020) 551–555.
[11] Z.J. Zhao, Z.L. Liu, Z.X. Zhu, Chin. Chem. Lett. 32 (2021) 2474–2478.
[12] S.H. Guo, J. Zhou, X. Zhao, J. Catal. 369 (2019) 201–208.
[13] W.L. Dai, W.W. Xiong, J.J. Yu, et al., ACS Appl. Mater. Interfaces 12 (2020) 25861–25874.
[14] J.W. Wang, W.K. Zhang, X.B. Zhang, et al., J. Alloy. Compd. 826 (2020) 154217.
[15] Y.S. Zeng, Q. Yin, Z. Liu, et al., Chem. Eng. J. 435 (2022) 134918.
[16] C.S. Li, X.S. Zou, W.H. Lin, et al., ACS Appl. Nano Mater. 4 (2021) 6280–6289.
[17] Y. Xiao, Z.Y. Peng, W.L. Zhang, et al., Appl. Surf. Sci. 494 (2019) 519–531.
[18] P. Wang, X.B. Zhou, Y. Shao, et al., J. Colloid Interface Sci. 601 (2021) 186–195.
[19] Q.K. Chen, L. Chen, J.J. Qi, et al., Chin. Chem. Lett. 30 (2019) 1214–1218.
[20] T.Y. Qiu, L. Wang, B.Y. Zhou, et al., ACS Appl. Nano Mater. 5 (2022) 702–709.
[21] F. Raziq, A. Hayat, M. Humayun, et al., Appl. Catal. B: Environ. 270 (2020) 118867.
[22] J.S. Han, F.X. Dai, Y. Liu, et al., Appl. Surf. Sci. 467 (2019) 1033–1039.
[23] S. Raheman AR, H.M. Wilson, B.M. Momin, et al., Renew. Energ. 158 (2020) 431–443.
[24] R.T. Guo, X.Y. Liu, H. Qin, et al., Appl. Surf. Sci. 500 (2020) 144059.
[25] V. Georgakilas, J.N. Tiwari, K.C. Kemp, et al., Chem. Rev. 116 (2016) 5464–5519.
[26] F. Li, D.K. Wang, Q.J. Xing, et al., Appl. Catal. B: Environ. 243 (2019) 621–628.
[27] D.R. Sun, S. Jang, S.J. Yim, et al., Adv. Funct. Mater. 28 (2018) 1707110.
[28] D.R. Sun, D.P. Kim, ACS Appl. Mater. Interfaces 12 (2020) 20589–20595.
[29] Y.W. Peng, M.T. Zhao, B. Chen, et al., Adv. Mater. 30 (2018) 1705454.
[30] Z.A. Zhong, L.S. Chen, L.S. Zhang, et al., Chin. Chem. Lett. 33 (2022) 3061–3064.
[31] L.F. Hong, R.T. Guo, Z.W. Zhang, et al., J. CO_2 Util. 51 (2021) 101650.
[32] X.L. Chen, Y. Cai, R. Liang, et al., Appl. Catal. B: Environ. 267 (2020) 118687.
[33] D.R. Sun, Y.H. Fu, W.J. Liu, et al., Chem. Eur. J. 19 (2013) 14279–14285.
[34] D.R. Sun, W.J. Liu, M. Qiu, et al., Chem. Commun. 51 (2015) 2056–2059.
[35] F.Y. Yu, X. Jing, Y. Wang, et al., Angew. Chem. Int. Ed. 60 (2021) 24849.
[36] H. Zhao, X. Yang, R. Xu, et al., J. Mater. Chem. A 6 (2018) 20152–20160.
[37] X.H. Jiang, Q.J. Xing, X.B. Luo, et al., Appl. Catal. B: Environ. 228 (2018) 29–38.
[38] Z.X. Pan, K. Zhao, J. Wang, et al., ACS Nano 7 (2013) 5215–5222.
[39] A. Hayat, T.A.M. Taha, A.M. Alenad, et al., Energy Technol 9 (2021) 2100091.
[40] J.W. Ren, S. Lv, S.Q. Wang, et al., Sep. Purif. Technol. 274 (2021) 118973.
[41] Z.K. Huang, H.J. Yu, L. Wang, et al., J. Hazard. Mater. 436 (2022) 129052.
[42] B. Ma, G. Chen, C. Fave, et al., J. Am. Chem. Soc. 142 (2020) 6188–6195.
[43] J.W. Ren, Y. Meng, X. Zhang, et al., Sep. Purif. Technol. 296 (2022) 121423.
[44] L.S. Zhang, X.H. Jiang, Z.A. Zhong, et al., Angew. Chem. Int. Ed. 60 (2021) 1–6.
[45] Z.L. Tang, C.J. Wang, W.J. He, et al., Chin. Chem. Lett. 33 (2022) 939–942.
[46] H.N. Che, P.F. Wang, J. Chen, et al., Appl. Catal. B: Environ. 316 (2022) 121611.
[47] X.H. Jiang, L.S. Zhang, H.Y. Liu, et al., Angew. Chem. Int. Ed. 59 (2020) 23112.
[48] D. Amarajothi, S.P. Andrea, M.A. Abdullah, et al., ChemCatChem 11 (2019) 899.